Structure of the Binuclear Metal-Binding Site in the GAL4 Transcription Factor†

Kevin H. Gardner, Tao Pan,‡ Surinder Narula, Edwin Rivera, and Joseph E. Coleman*
Department of Molecular Biophysics and Biochemistry, Yale University, New Haven, Connecticut 06510
Received June 17, 1991; Revised Manuscript Received September 5, 1991

ABSTRACT: The GAL4 transcription factor from yeast contains within its N-terminal DNA-binding domain an amino acid sequence containing six cysteine residues, C11-X_2-C14-X_6-C21-X_6-C28-X_2-C31-X_6-C38. The six Cys residues will form a binuclear metal cluster with either Zn(II) or Cd(II) in which two of the $-S^-$ donors are bridging ligands between the two metal ions. Binding of Zn(II) or Cd(II) to the GAL4 DNA-binding domain is essential to induce the conformation of GAL4 required for the protein to recognize the specific DNA sequence, UAS_G, to which GAL4 binds. Evidence for the presence of the binuclear cluster has come from ^{113}Cd NMR and 2D ^1H–^{113}Cd heteronuclear NMR studies of the cloned DNA-binding domain of GAL4 consisting of the N-terminal 62 residues, GAL4(62*) [Pan and Coleman (1990) *Proc. Natl. Acad. Sci. U.S.A. 87*, 2077]. Cd(II) binding to the GAL4 DNA is highly cooperative, thus the Cd_2Cys_6 cluster is always formed. On the other hand, Zn(II) forms well-defined Zn_1 and Zn_2 complexes with the DNA-binding domain of GAL4, both of which bind specifically to the UAS_G DNA sequence. The structural details of the Cd_2-, Zn_2-, and Zn_1GAL4(62*) proteins have been determined by a variety of heteronuclear and 2D NMR techniques. When Cd(II) is exchanged for Zn(II), the cluster appears to expand to accommodate the larger Cd(II) ion as suggested by changes of 2 to 4 Hz in the $^3J_{HN\alpha}$ coupling constants for the amino acid residues which form the polypeptide loops enclosing the cluster, residues 10–40. These changes suggest alterations in the backbone ϕ torsional angles of from 20° to 30°. A metal–ligand structure derived from the ^1H–^{113}Cd heteronuclear NMR as well as the polypeptide backbone connectivity around the cluster as determined from short-range ^1H–^1H NOE's is presented. The metal ions also determine the major folding of GAL4(62*), since the chemical shift dispersion in the entire NH–αCH fingerprint region of the ^1H–^1H COSY spectrum collapses on removal of the metal ion. Two short segments of the GAL4(62*) polypeptide (residues 14–19 and 30–36 in the cluster forms, 12–19 and 30–36 in the Zn_1 species) show significant dNN(i,i+1) NOE's. These short segments of polypeptide chain are the only ones that could be helical in the GAL4(62*). These NOE's show significant differences in magnitude relative to the αN(i,i+1) NOE's for the same residues between the Cd_2 and Zn_2 proteins as well as between the Zn_2 and Zn_1 proteins. Thus both the species of metal ion [Zn(II) or Cd(II)] and the number of metal ions bound determine the conformation of the peptide backbone.

GAL4 protein is a transcription factor from *Saccharomyces cerevisae* required for the transcriptional activation of the genes encoding the galactose-metabolizing enzymes in response to galactose [for review, see Giniger et al. (1985) and Johnston (1987a)]. The protein of 881 amino acids binds as a dimer to a 17 bp palindromic DNA sequence known as the UAS_G, which is present in one to four copies upstream of the inducible genes. In the absence of galactose, GAL4 appears to remain bound to the UAS_G sequence but is inactivated by formation of a complex with another protein, GAL80 (Johnston et al., 1987; Ma & Ptashne, 1987). In the presence of galactose, a metabolite derived from galactose binds to GAL80, dissociating the GAL80 protein and thus allowing GAL4 to activate transcription. The DNA-binding domain of GAL4 is located in the N-terminal 62 residues and includes a sequence, -C11-X_2-C14-X_6-C21-X_6-C28-X_2-C31-X_6-C38-, conserved among 13 other fungal transcription factors (Keegan et al., 1986; Pfeifer et al., 1989; Marczak & Brandriss, 1991). This Cys-rich sequence initially suggested that GAL4 was a Zn(II)-containing transcription factor containing a "zinc-finger" motif as originally described for TFIIIA (Johnston, 1987b). Analytical data, however, showed that up to two metal ions, either Zn(II) or Cd(II), could bind to the 62-residue N-terminal subdomain of GAL4, GAL4(62*) (Pan & Coleman, 1990a,b). The presence of Zn(II) or Cd(II) was demonstrated to be essential for specific binding of GAL4 to the UAS_G sequences (Pan & Coleman, 1989).

Both ^{113}Cd NMR and ^1H–^{113}Cd coupling observed in 2D ^1H–^1H COSY spectra of $^{113}Cd_2$GAL4(62*) have shown that the six Cys residues are the only ligands to the two ^{113}Cd ions (Pan & Coleman, 1990a, 1991). The chemical shifts of the ^{113}Cd resonances, however, 707 and 669 ppm, implied that both ^{113}Cd(II) ions are coordinated to four sulfur donors (Pan & Coleman, 1989, 1990a). This led to the suggestion that two of the six Cys were bridging ligands to both metal ions, forming a binuclear metal cluster (Pan & Coleman, 1989). Complete 2D ^1H COSY and ^1H NOESY NMR spectra have been collected on Zn(II)$_2$GAL4(62*) and Cd(II)$_2$GAL4(62*), and the short-range and long-range NOE data have been used to calculate a low-resolution three-dimensional solution structure (Pan & Coleman, 1991). We previously suggested that the bridging cysteines were C21[1] and C31 on the basis of the

† This work was supported by NIH Grants DK09070 and GM21919. The 500-MHz NMR facility was supported by NIH Grant RR03473, NSF Grant DMB-8610557, and ACS Grant RD259. K.H.G. is supported by a predoctoral fellowship from the Howard Hughes Medical Institute. This work is in partial fulfillment of the Ph.D. requirements for K.H.G. S.N. is supported by NIH Grant DK18778.
* Corresponding author.
‡ Current address: Department of Chemistry and Biochemistry, University of Colorado, Boulder, CO, 80309.

[1] Correction: In the original sequential assignment of GAL4(62*) (Pan & Coleman, 1991), R15 was misassigned. Thus the essentially palindromic sequence of spin systems, C14-R-L-K-K-L-K-C21, was assigned in reverse. The correct connectivity is shown here in the more highly resolved NOESY spectra shown in Figures 6–8.

0006-2960/91/0430-11292$02.50/0

patterns of ^1H–^{113}Cd coupling observed in the β^a–β^b cross peaks of the COSY spectra (Pan & Coleman, 1990b). Two-dimensional heteronuclear double-quantum ^1H–^{113}Cd COSY spectra, however, show that the bridging residues are C11 and C28 (Pan & Coleman, 1991). The proton NMR data alone, however, do not supply information on the precise molecular topology of the binuclear complex. In fact, when calculating the 3D structure, one has to assume initially that the binuclear site is made up of two approximately tetrahedral metal complexes fused along one edge. While the tetrahedral bond angles and bond lengths, taken from model complexes or metallothionein (Robbins et al., 1991), can be either restrained or allowed to drift during the energy minimization program used to calculate the 3D structure, little additional detailed information can be gained as to the structural details of the binuclear metal center.

The present paper describes an investigation of the binuclear metal complex using the $^{113}Cd(II)$ ion as the probe and employing relaxation data, 2D heteronuclear double-quantum correlation spectroscopy, ^{113}Cd-filtered ^1H–^1H COSY difference spectroscopy, and ^1H–^{113}Cd coupling patterns to delineate the detailed architecture of this unusual binuclear metal complex. The binding of Cd(II) to GAL4 is highly cooperative, and only the two-metal cluster forms. In contrast, the native Zn(II) forms a well-defined Zn_1 as well as a Zn_2 derivative. The wrapping of the polypeptide around the metal ion(s) is the major determinant of the structure of the DNA-binding domain of GAL4. Therefore, knowledge of the details of the coordination chemistry surrounding the metal ions is essential for the determination of the complete solution structure of this protein domain.

Materials and Methods

Preparation of $Zn(II)_2$- and $^{113}Cd(II)_2$GAL4(62).* Cloning, overexpression, and purification of GAL4(62*) from *E. coli* have been described previously (Pan & Coleman, 1989, 1990b). The $Zn(II)_2$GAL4(62*) was prepared by dialysis of 2 mM native protein against 4 mM $ZnCl_2$, pH 5.4. All the samples used for NMR were contained in 50 mM sodium phosphate/100 mM NaCl unless otherwise stated. The $Cd(II)_2$GAL4(62*) was prepared by incubation of the zinc protein in a 3-fold excess of $^{113}CdCl_2$ over protein in the standard buffer at room temperature for 12 h, followed by dialysis to remove the displaced Zn(II). The Cd(II) for Zn(II) exchange is most rapid at pH 5.0. The procedure was generally repeated twice to ensure removal of all the Zn(II). The sample of $^{113}Cd_2$GAL4(62*) used for the studies at pH 8.0 was 3 mM. Because of its lesser stability, we did not prepare samples of the zinc protein below pH 5.4. The sample of $^{113}Cd_2$GAL4(62*) used in the HMQC and ^{113}Cd filter experiments was 15 mM at pH 6.0 and was concentrated by lyophilization followed by redissolving in 90% H_2O/10% D_2O with appropriate adjustments of buffer and salt concentration before or after lyophilization.

Protein Concentrations. Protein concentrations were routinely determined by amino acid analyses, since optical density at 280 nm presents some practical problems in the case of GAL4(62*). The amino acid sequence contains one Trp and one Tyr, and the extinction coefficient of the indole ring is sensitive to the presence of the metal ion(s). In addition, the Cd(II) protein has intense $-S^- \rightarrow Cd$ charge transfer bands which overlap the near-UV chromophores of the protein. We have nevertheless determined as accurately as possible the ϵ_{280nm} for three species of GAL4(62*), and they are $Zn_2 = 7.8 \times 10^3$ M^{-1} cm^{-1}, $Cd_2 = 11 \times 10^3$ M^{-1} cm^{-1}, and apoGAL4(62*) $= 9.8 \times 10^3$ M^{-1} cm^{-1}.

^1H NMR, ^1H–^{113}Cd, and ^{113}Cd-Filtered ^1H NMR. NMR experiments were performed on a Bruker (Billerica, MA) AM-500 spectrometer at 35 °C. All samples were stored under nitrogen to prevent oxidation of the SH groups. Inverse detection experiments (^1H–^{113}Cd double-quantum correlation spectra and ^{113}Cd-filtered ^1H COSY spectra) used a 5-mm inverse broad band tunable probe. Chemical shifts are plotted relative to sodium (trimethylsilyl)tetradeuteriopropionate. The FID data were transferred to a Sun Sparc 2 workstation, and the FELIX program of Dennis Hare (Hare Research, Woodinville, WA) was used for processing the 2D NMR spectra. Spectral parameters and pulse sequences are described in the figure captions. The carrier was placed in the center of the spectrum on the water signal, and a recycle delay of 1.5–2.0 s was used. During the recycle delay and the mixing time, the water signal was suppressed by continuous low-power irradiation from the proton decoupler channel. The spectral width F_2 was 5681.8 Hz, and 512 increments (64 scans each) were collected with 2048 data points. The F_1 domain was subsequently zero-filled to 2048 points prior to Fourier transformation (real) to provide 2048 (F_2) × 1024 (F_1) final matrices. Fourier transformation in both dimensions was performed after multiplication by a sine-squared window function with 10° and 40° phase shifts for COSY and NOESY spectra, respectively. Structures of the GAL4 metal cluster were calculated by entering the NOESY-determined interproton distances, backbone torsional angles, ϕ, calculated from $^3J_{HN\alpha}$ coupling constants, and the constraints provided by the binuclear Cd(II) complex into the energy minimization program XPLOR (Brunger, 1990).

^{113}Cd NMR. ^{113}Cd NMR was performed on a Bruker AM-500 spectrometer at 25 °C using a frequency of 110.9 MHz for ^{113}Cd. A 10-mm tunable broad band probe was used. The spectral width was 15.2 kHz (136 ppm). The pulse angle was 45°, and a delay time of 2 s was used. The $^{113}Cd_2$GAL4(62*) sample was 4 mM in protein, contained in 1.8 mL of either 40 mM Tris, pH 8.0, or 50 mM phosphate, pH 5.0. For the inversion–recovery method of measuring T_1, a 15 mM protein sample, pH 6.0, was used with an inverse broad band tunable probe.

Results

^{113}Cd NMR of $^{113}Cd(II)$GAL4(62).* A cloned and overproduced subfragment of GAL4 constituting the entire DNA-binding domain has been described previously (Pan & Coleman, 1990a,b). This fragment, known as GAL4(62*), constitutes the first 62 N-terminal residues of GAL4 except that residue 62 is changed from Glu 62 to Asp 62. The ^{113}Cd NMR spectrum of $^{113}Cd(II)_2$GAL4(62*) is presented in Figure 1 in the form of a standard inversion–recovery sequence for measuring the T_1 values of the two ^{113}Cd nuclei. Because of the insensitivity of the ^{113}Cd nucleus, relatively little data exist in the literature on relaxation of ^{113}Cd in protein sites. This experiment utilized a 15 mM $^{113}Cd(II)_2$GAL4(62*) sample at pH 6.0. The T_1 values for the two ^{113}Cd nuclei are approximately equal with rapid relaxation times, ~0.1 s.

^1H–^1H COSY Spectroscopy of $^{113}Cd_2$GAL4(62) Using ^{113}Cd Filters.* As described by Wörgötter et al. (1986) and Otting and Wüthrich (1990), protons coupled to a heteronucleus can be singled out in a complex ^1H–^1H COSY spectrum by the use of X-filters (X = heteronucleus). Formation of a COSY difference spectrum removes all cross peaks and diagonal peaks not coupled to the heteronucleus. A ^1H–^1H COSY difference spectrum employing a ^{113}Cd single filter is shown in Figure 2A and consists of the resonances of the β protons of the six C residues of GAL4(62*) on the diagonal

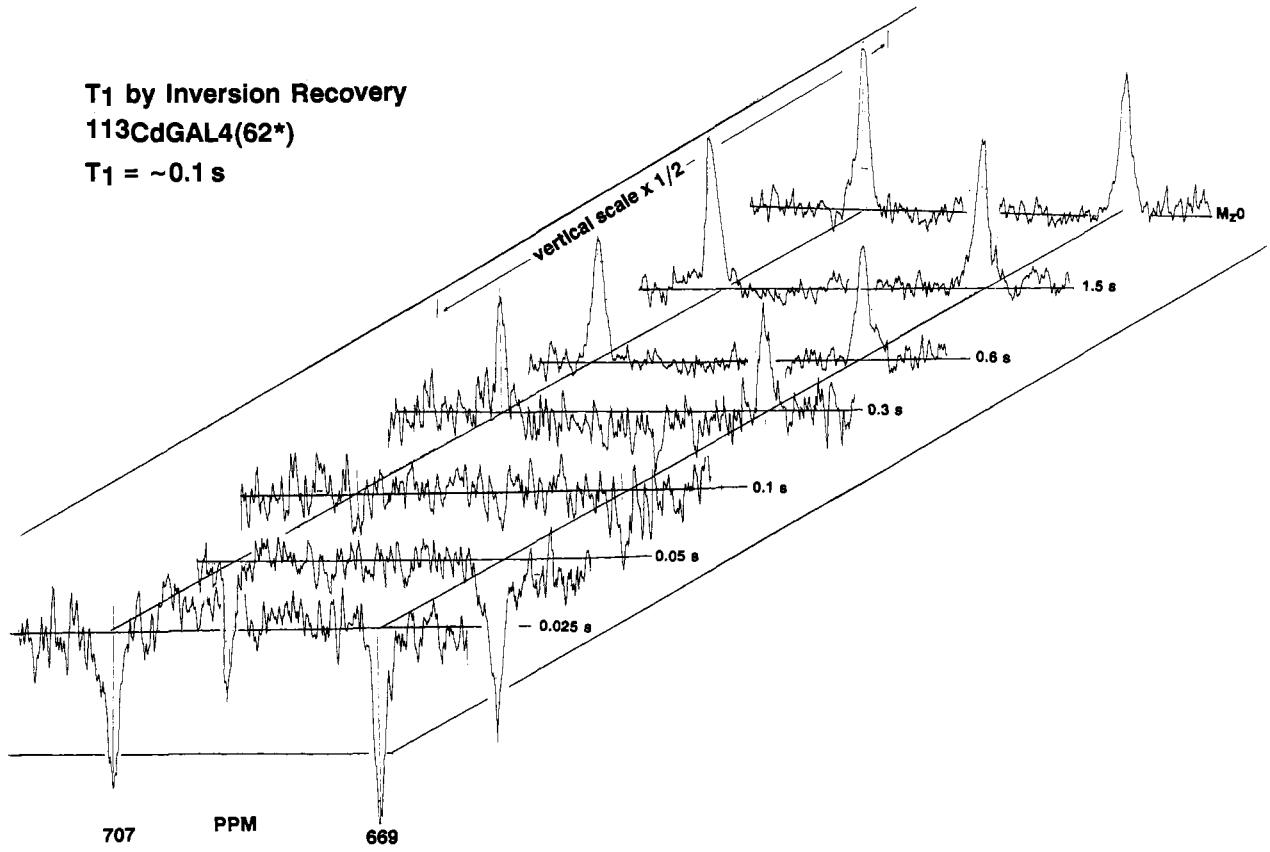

FIGURE 1: Determination of the T_1 relaxation of the two ^{113}Cd nuclei in ^{113}Cd$_2$GAL4(62*) by the inversion–recovery method. The sample was 15 mM in protein, pH 6.0, and the spectrum represents 512 scans.

and their $\beta^a\beta^b$ COSY cross peaks. These are the only signals in the spectrum and graphically confirm the earlier conclusion, based on the coupling seen in a normal ^{1}H–^{1}H COSY spectrum, that the six Cys residues are the only residues contributing ligands to the two ^{113}Cd ions (Pan & Coleman, 1990b).

The use of a ^{113}Cd double filter can detect those protons which are coupled to two ^{113}Cd nuclei, even if the coupling constant to the second ^{113}Cd is small. A ^{1}H–^{1}H COSY difference spectrum with the two ^{113}Cd filter in place is shown in Figure 2B. While weak, the only cysteine $\beta^a\beta^b$ cross peaks remaining are those of C11 and -28, suggesting that the $-S^-$ from these two residues form the bridging ligands.

Two-Dimensional ^{1}H–^{113}Cd Double-Quantum Correlation (HMQC) Spectra. A second means of detecting the bridging Cys residues in a binuclear cluster is to perform a 2D double-quantum ^{1}H–^{113}Cd correlation experiment (Neuhaus et al., 1984; Frey et al., 1985; Norwood et al., 1990). Contour plots of 2D ^{1}H–^{113}Cd HMQC experiments on ^{113}CdGAL4(62*) are shown in Figure 3, panels A and B. Conditions for the two experiments differ in the following ways. The τ value ($1/2J$) for the spectrum of Figure 3A was set at 10 ms, expected to emphasize proton resonances whose ^{1}H–^{113}Cd coupling constants are ~50 Hz, while the τ value of Figure 3B was 50 ms, expected to emphasize proton resonances whose ^{1}H–^{113}Cd coupling constants are 10 Hz or less. In order to enhance the signal-to-noise ratio of the latter spectrum, the phase-alternated third ^{113}Cd ($\pi/2$) pulse and preceding delay time were eliminated. Thus the resonances of Figure 3B have alternating phases. The β proton assignments given in Figure 3A are from ^{1}H–^{1}H COSY experiments and the previous sequential assignments of GAL4(62*) (Pan & Coleman, 1990b, 1991) with the exception of C14 and -21.[1] The chemical shifts of the NH, αH, and βH protons of the six cysteine residues as well as the ^{1}H–^{113}Cd coupling constants for each of the β protons as determined from ^{1}H–^{1}H COSY spectra are summarized in Table I.

The 2D HMQC spectra show that the Cys residues fall into two groups of three based on strong coupling to one or the other of the two ^{113}Cd ions. The β protons of C11, -14, and -21 are most strongly coupled to the ^{113}Cd ion resonating at 669 ppm, while those of C28, -31, and -38 are most strongly coupled to the ^{113}Cd ion resonating at 707 ppm (Figure 3A,B). As expected, the β protons of C21 and C38, with $^3J_{\beta Cd}$ of 55 Hz, are strongly represented in Figure 3A. The overlap of strong resonances in the center of this 2D spectrum due to similar chemical shifts for several of the β protons makes it difficult to be certain whether the β protons of C11, -14, and -21 are coupled to both ^{113}Cd ions or not.

In Figure 3B, with τ = 50 ms, all cysteine β protons except those of C21 and C38 are more strongly represented as expected from their smaller $^3J_{\beta Cd}$ couplings. In addition, the weak couplings expected between the β protons and the second ^{113}Cd in the case of bridging cysteines, are brought out, i.e., the β protons of bridging residues will be represented in the contour plots at the ω_2 positions for both ^{113}Cd resonances. The $-S^-$ of C28 is clearly a bridging ligand as is the $-S^-$ of C11. Both β protons of C28 are about equally coupled to the second ^{113}Cd, while β^a of C11 is much more strongly coupled to the second ^{113}Cd than β^b of this residue (Figure 3B). From the data in Figure 3B, C21 and C38 can be eliminated as bridging ligands. The β^b protons of both C14 and -31 are not coupled to a second ^{113}Cd ion (Figure 3B). The overlap of the β^b protons of C14 and C31 makes it difficult to eliminate the possibility of coupling of these protons to both ^{113}Cd ions, but the fact that they are absent in the ^{113}Cd double-filter experiment eliminates this possibility (Figure 2B).

^{1}H–^{113}Cd Heteronuclear Coupling As Observed in the ^{1}H–^{1}H COSY of GAL4(62).* In the case of metallothionein, the

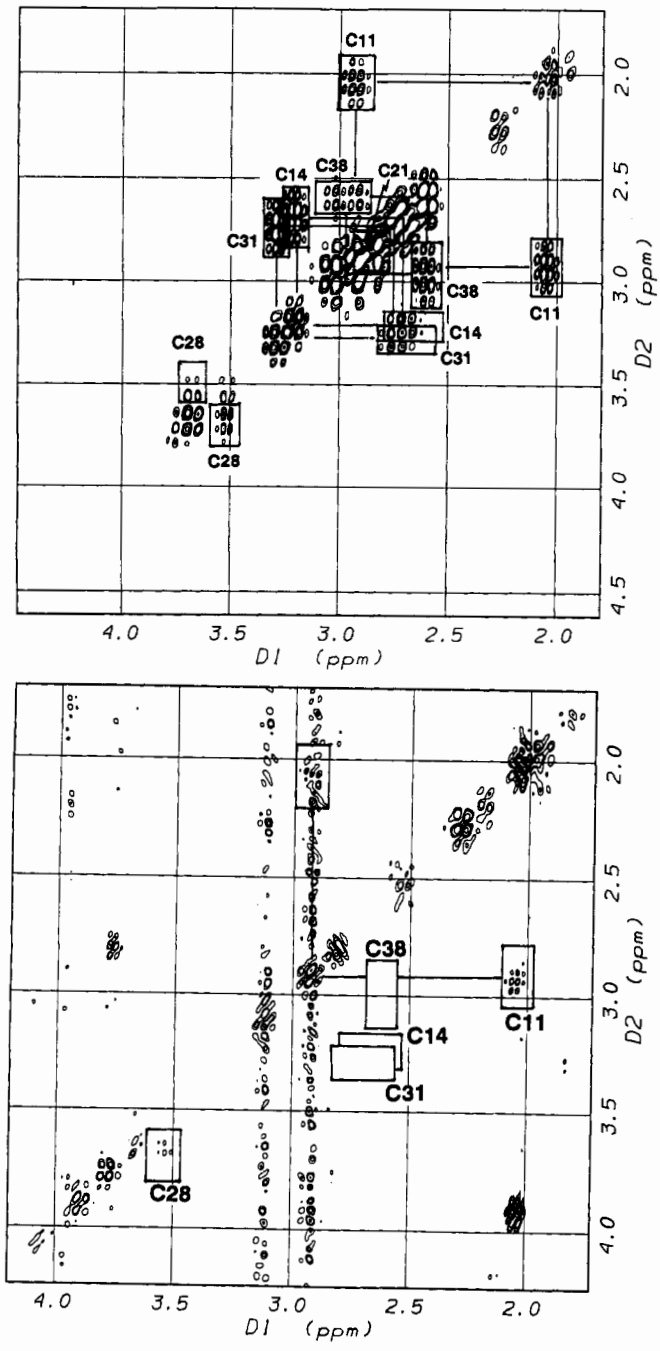

FIGURE 2: ^{113}Cd-filtered 2D ^{1}H COSY difference spectra. (A, top) Single ^{113}Cd-filtered spectrum (256 scans per experiment, 300 experiments, 5681.8 Hz sweep width, t_1^{max} = 26.0 ms). (B, bottom) Double ^{113}Cd-filtered spectrum (128 scans per experiment, 320 experiments, 3496.5 Hz sweep width, t_1^{max} = 45.8 ms). The sample is the same as in Figure 1.

previous IIB metal ion cluster-containing protein found in nature, two of the eight bridging Cys residues were identified from characteristic heteronuclear coupling patterns observed for the $\beta^a\beta^b$ cross peaks in the ^{1}H–^{1}H COSY of a ^{113}Cd-substituted protein (Neuhaus et al., 1984, 1985). The $\beta^a\beta^b$ COSY cross peaks for ligands C11 and -28 (definitely bridging ligands from the HMQC experiments) and C14[1] and -31 are shown in Figures 4 and 5 for both $^{112}Cd_2$ and $^{113}Cd_2$ derivatives of GAL4(62*). In the case of C14 and -31, representative spectra are given for both pH 8.0 and 6.0. NOESY spectra for Cd_2GAL4(62*) are similar at pH 6.0 and 5.0. The latter is the pH at which the sequential assignment was carried out (Pan & Coleman, 1991). The β protons of C11, -14, -28, and -31 are all strongly coupled to one of the two Cd(II) ions, J varying from 10 to 55 Hz. In general β^a is more strongly coupled than β^b (Figures 4 and 5, Table I).

We had thought originally that in the $\beta^a\beta^b$ cross peaks of C14[1] and C31 there was evidence of small coupling to the second ^{113}Cd, since there do appear to be small increases in center-to-center peak distances between the ^{112}Cd and ^{113}Cd spectra (Figure 4). On the other hand, the $\beta^a\beta^b$ coupling patterns for residues C11 and C28, which the 2D HMQC show to be bridging ligands, show no additional evidence of coupling to the second ^{113}Cd (Figure 5). The failure to detect the weak coupling to the second ^{113}Cd ion from the $\beta^a\beta^b$ cross peaks may be due to the small magnitude of the coupling of the bridging cysteines to the second ^{113}Cd. The coupling patterns, like the chemical shifts of the ^{113}Cd signals, are independent of pH from 8.0 to 6.0 (Figure 4C). The overlap of the patterns for C14 and C31 at pH 6.0 is due to a 0.04 ppm upfield shift of the β^b proton of C31, at the lower pH. The NN, αN, and βN NOE patterns for both Zn_2- and $^{113}Cd_2$GAL4(62*) suggest that the two metal derivatives assume very similar although not identical structures (Pan & Coleman, 1991) (see Figures 6–8 below). The β protons of the cysteine residues in the Zn_2GAL4(62*) at pH 5.4 show very similar chemical shifts and ^{1}H–^{1}H coupling constants to those of the Cd_2GAL4(62*) at either pH 8.0 or 6.0 (Table I).

Changes in the Structure of GAL4 on the Substitution of Cd(II) for Zn(II). Most of the details of the binuclear cluster found in the DNA-binding domain of GAL4 have been worked out using the $^{113}Cd_2$ derivative because of the major additional information available from the heteronuclear ^{1}H–^{113}Cd coupling as outlined above. Both the Cd(II) and Zn(II) proteins bind to the specific UAS_G DNA sequence recognized by GAL4 (Pan & Coleman, 1989); nevertheless, Zn(II) is the native metal ion, and zinc and cadmium coordination chemistry, especially with sulfur, are not always identical. Many more Cd(II)–sulfur cluster compounds have been described than Zn(II) clusters, and the Cd–S bond averages 2.5 Å rather than 2.3 Å characteristic of Zn–S bonds.

As we have shown previously, it is possible to form a Zn_2GAL4(62*) complex with ^{1}H–^{1}H COSY and NOESY spectra generally similar to those of Cd_2GAL4(62*) (Figures 6 and 7; Pan & Coleman, 1991). It is important, however, to document in detail the extent to which the structures of the two metalloproteins differ in order to evaluate the tacit assumption that both derivatives will allow similar structure–function conclusions to be made. As we noted earlier when carrying out the sequential assignments of the Zn(II) and Cd(II) proteins, there are significant chemical shift changes in a number of the backbone amide protons, and some αCH and βCH protons as well, consequent to the Cd(II) substitution (Pan & Coleman, 1991).

αNH and βNH NOESY Spectra Documenting the Sequential Assignments through the Cysteine Cluster of $^{113}Cd_2$GAL4(62).* To document the sequential assignments of GAL4(62*) in the region of the cluster of six cysteine residues and the relative magnitudes of the various NOE's, the NOESY spectrum obtained on the 15 mM sample of $^{113}Cd_2$GAL4(62*) used for the ^{113}Cd filter spectra and the HMQC spectra is shown in Figure 6. The spectrum was collected at a τ value of 150 ms in a sequence of spectra taken at τ values of 30, 60, 100, and 150 ms to measure the NOE growth curves. The NOESY cross peaks used in the sequential assignment all have growth curves appropriate for primary NOE's. In this spectrum, i to i+1 connectivity relevant to the Cys residues extends for the αN NOEs from residues 8–12,

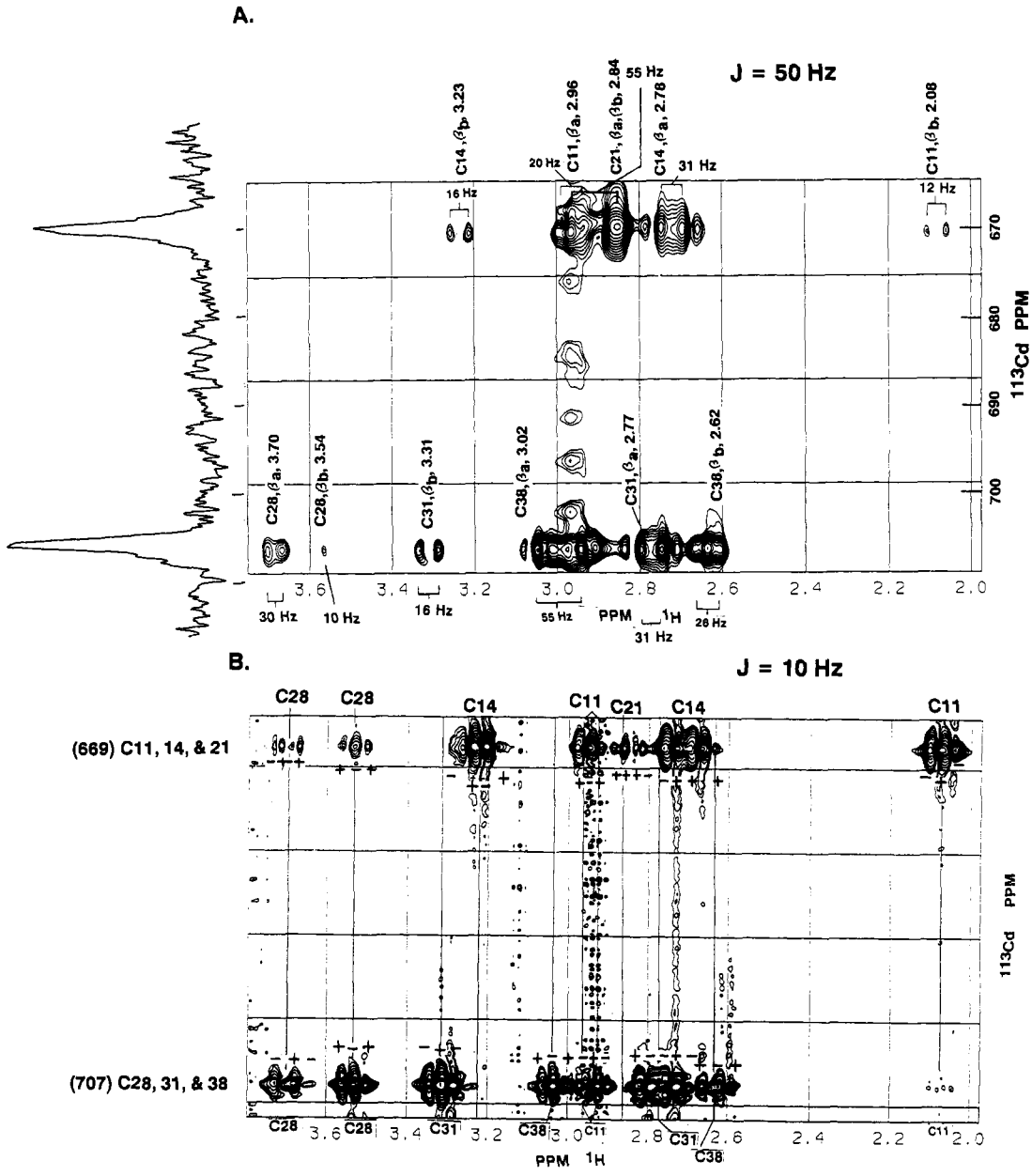

FIGURE 3: Heteronuclear ^1H–^{113}Cd COSY spectrum of ^{113}CdGAL4(62*). The pulse sequences employed are as described in Norwood et al. (1985). (A) The delay time, $\tau = 1/2J$, was set at 10 ms, corresponding to a ^1H–^{113}Cd coupling constant of 50 Hz. (B) The delay time τ was set at 50 ms, corresponding to a ^1H–^{113}Cd coupling constant of 10 Hz. The insertion of an additional delay time and the phase-alternated $^{113}Cd(\pi/2)$ pulse, which eliminates antiphase proton coherence with respect to heteronuclear couplings, was removed in part B to improve the signal-to-noise ratio. The protein sample was 15 mM, pH 6.0, 35 °C.

14–19, and 26–39 and for the βN NOE's from residues 10–12, 14–17, 19–21, 26–37, and 40–41. In both sets of NOE's, the connectivities are sufficient to establish the unique assignments for five of the six cysteine residues. One of them, assigned to C21 by exclusion, gives no readily identifiable connectivity, only a single cross peak whose partner is not easily identified (Figure 6). This lack of close contact of C21 with adjacent residues seems to be supported by the degeneracy of its βCH protons (Table I).

Although there are significant chemical shift changes between the Cd_2 and Zn_2 forms of GAL4(62*), the patterns of αN backbone NOE's are similar enough to suggest that the two conformations are related. The NOESY spectrum for the Zn_2GAL4(62*) in the region of the αN NOESY cross peaks is shown in Figure 7, and the backbone connectivity can be compared with that derived from the αN NOE's of the Cd_2GAL4(62*). In both Zn_2GAL4(62*) and Cd_2GAL4(62*) one $i,i+3$ NOE is present between N35 and L32.

NH–NH NOESY Spectra for Three Forms of GAL4(62), Zn_2GAL4(62*), Cd_2GAL4(62*), and Zn_1 GAL4(62*).* We have found three relatively stable metalloforms of GAL4(62*). Both Cd(II) and Zn(II) form species containing two metal ions as presented above. Binding of two Cd(II) ions to GAL4(62*) is sufficiently cooperative that the Cd_2–protein is the only species formed at equilibrium. In contrast, one of the Zn(II) ions can be readily removed from the Zn_2 protein by dialysis against metal-free buffer as previously documented (Pan & Coleman, 1989, 1990a). The Zn_1 and Zn_2 derivatives of GAL4(62*) are both stable and have substantially different conformations as indicated by significant changes in the chemical shifts of a number of NH resonances as well as significant changes in the magnitudes and pattern of their NN and αN NOE's.

The NH–NH NOESY spectra for the two binuclear metal cluster derivatives of GAL4(62*) and the derivative containing a single zinc ion are compared in Figure 8. Two stretches

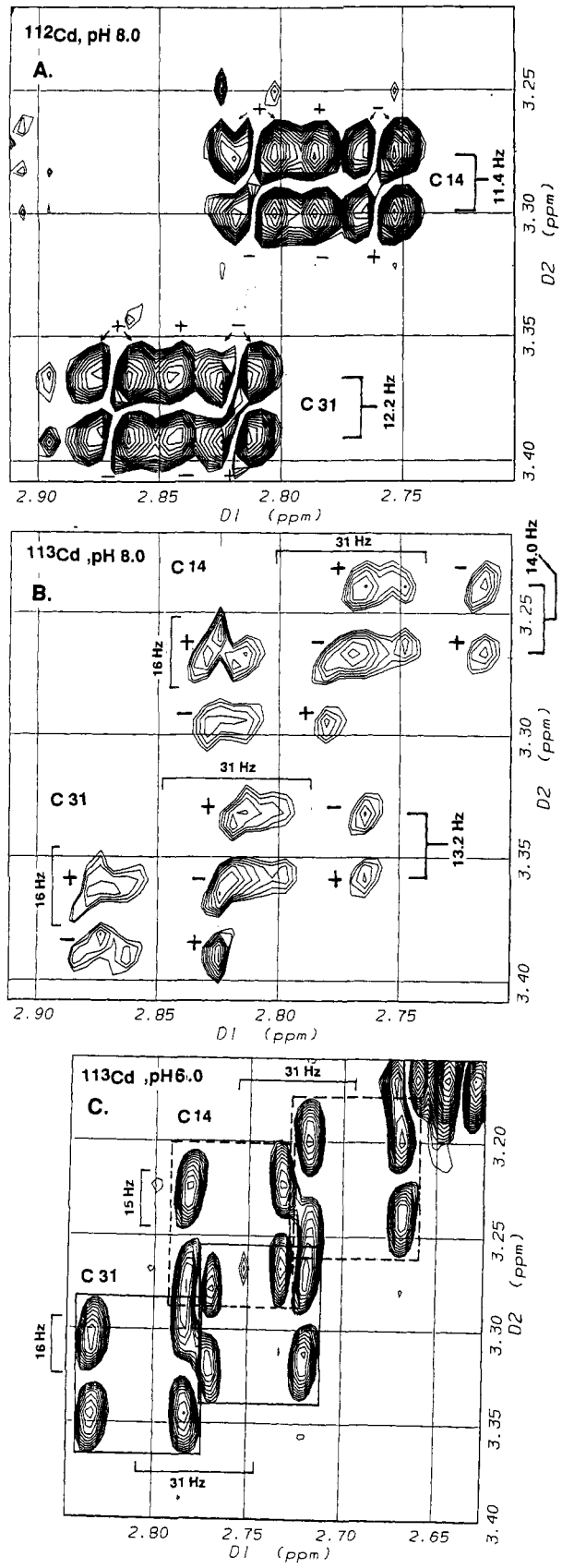

FIGURE 4: The $\beta^a\beta^b$ DQF ^1H COSY cross peaks for C14 and C31 in $^{112}Cd_2$GAL4(62*), pH 8.0, 35 °C (A); $^{113}Cd_2$GAL4(62*), pH 8.0, 35 °C (B); and $^{113}Cd_2$GAL4(62*), pH 6.0, 35 °C (C). The protein concentration in parts A and B was 3 mM and that in part C was 15 mM. For all the ^1H–^1H COSY experiments, the sweep width was 2790 Hz with 2048 data points in the t_2 domain and 512 experiments in the t_1 domain. The relaxation delay was 1.7 s. Assignments of the coupling constants marked by brackets in Figures 3 and 4 are given in Table I.

of polypeptide chain, one in the N-terminal end of the Cys-rich cluster (residues 14–19 in the binuclear forms and 12–19 in the Zn_1GAL4(62*) and one in the C-terminal region of the Cys-rich cluster (residues 30–36 in all three metal derivatives) have signifcant $i,i+1$ NOE's (Figure 8). There are significant changes in both the magnitudes and the pattern of NN NOE's among the three derivatives. Thus all three derivatives appear to have significantly different conformations, especially in the stretch of polypeptide chain between C11 and C21. The differences in conformation along the polypeptide backbone are also indicated by significant differences in coupling constants, $^3J_{HN\alpha}$, throughout the segment of the polypeptide chain forming the binuclear cluster in the two metal derivatives of GAL4(62*) (Figure 9).

Discussion

We originally postulated the presence of a binuclear metal cluster in the DNA-binding domain of GAL4 based on the presence of two downfield (669 and 707 ppm) ^{113}Cd resonances, each integrating to one ^{113}Cd nucleus and observed for the $^{113}Cd_2$ derivatives of both GAL4(149*) and GAL4-(62*) (Pan & Coleman, 1989, 1990a,b). Since the only amino acid residues involved in ligation to the two ^{113}Cd ions were the six Cys residues, we postulated that two of the cysteines must be bridging ligands. The pattern of primary $^1H_\beta$–^{113}Cd couplings revealed by the HMQC experiment (C11, -14, and -21 coupled to the ^{113}Cd ion resonating at 669 ppm and C28, -31, and -38 coupled to the ^{113}Cd ion resonating at 707 ppm) confirms an independent observation from the NOESY spectra for both Zn_2- and Cd_2GAL4(62*) (Pan & Coleman, 1991). That observation is that the NH proton of C11 shows NOE's to the β protons of C14 and -21, while the NH proton of C28 shows NOE's to the β protons of C31 and -38, suggesting a division into two closely spaced groups of three Cys residues each (Pan & Coleman, 1991). One might even raise the issue of whether two trigonal $^{113}Cd(II)$ complexes might be a reasonable description of the complex. While the coupling through the bridging $-CH_2-S^-$ to the second ^{113}Cd ion is relatively weak (Figures 2B and 3B), the downfield chemical shifts of both ^{113}Cd ions are compatible with S_4 rather than S_3 coordination. That the six cysteine residues are the only ligands to the two $^{113}Cd(II)$ ions is confirmed by the ^1H–^1H COSY difference spectrum employing a ^{113}Cd filter (Figure 2A).

The fact that when a bridging cysteine is present, one of the two ^{113}Cd nuclei is much more strongly coupled to the β protons than the other was well documented in the case of the $^{113}Cd_7$ metallothionein (Neuhaus et al., 1984; Wüthrich, 1986). In the latter case, the best example of a bridging cysteine had primary ^1H–^{113}Cd coupling to the β protons of ~40 Hz, while the ^1H–^{113}Cd coupling to the second ^{113}Cd was ~12 Hz. While the small binuclear complex of GAL4 does have some primary ^1H–^{113}Cd couplings as large as 50 Hz (Table I), the β protons of the bridging ligands have no primary ^1H–^{113}Cd couplings greater than ~25 Hz (Table I). The small couplings to the second ^{113}Cd, ~5 Hz, do not show up except in the HMQC spectra (Figure 3B). The couplings to the second ^{113}Cd shown by the bridging ligands are also detectable by the ^1H–^1H COSY difference spectrum employing a ^{113}Cd double filter, which supports the assignment of C11 and -28 as the only bridging ligands (Figure 2B).

The ligand distribution and the connectivity of the polypeptide backbone around the binuclear Cd(II) cluster of GAL4 taken from the current refinement of the 3D solution structure of the Cd_2(GAL4(62*) is schematically illustrated in Figure 10. Determination of the precise polypeptide connectivity

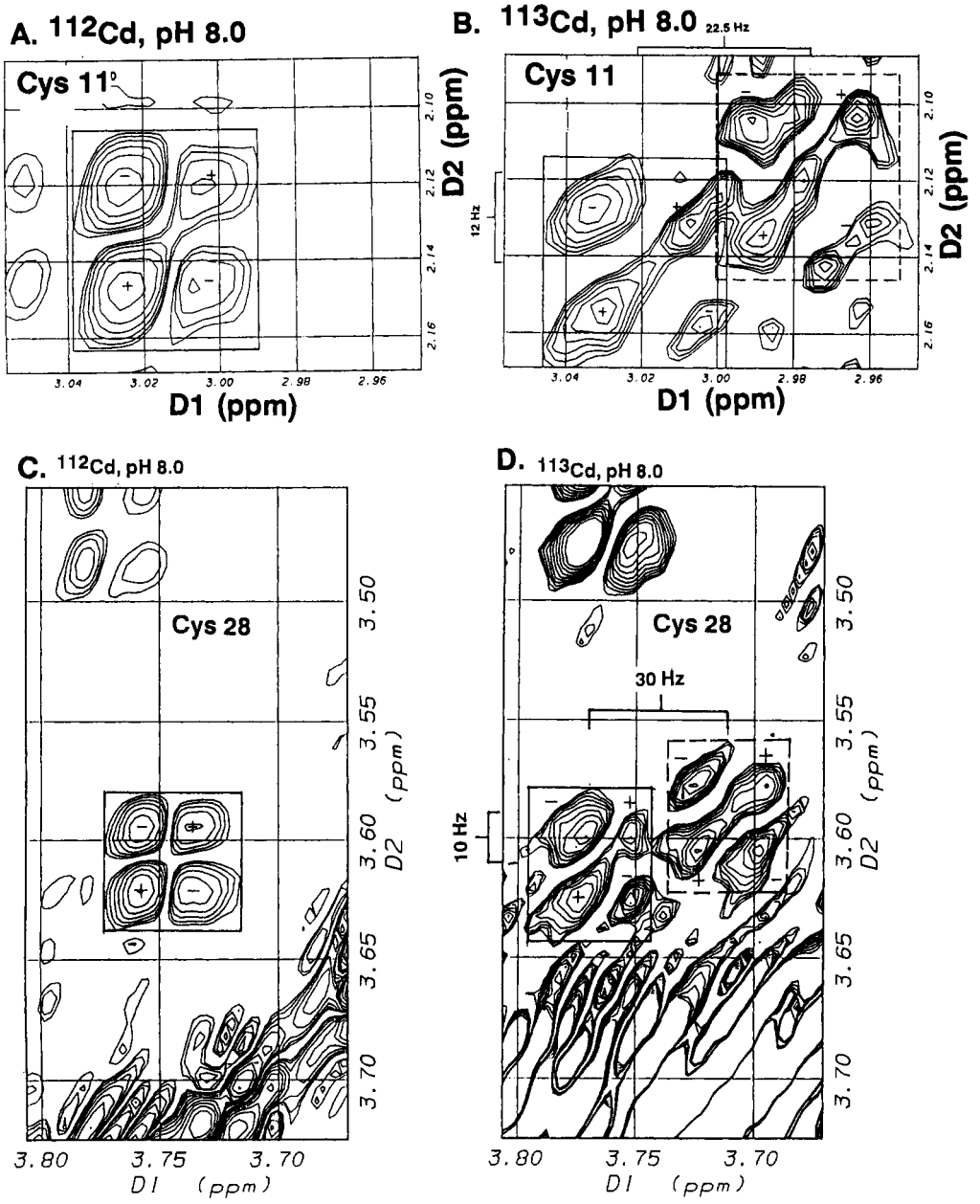

FIGURE 5: The $\beta^a\beta^b$ DQF ^{1}H COSY cross peaks for C11 and C28 in $^{112}Cd_2$GAL4(62*) and in $^{113}Cd_2$GAL4(62*). (A) C11, ^{112}Cd, pH 8.0. (B) C11, ^{113}Cd, pH 8.0. (C) C28, ^{112}Cd, pH 8.0. (D) C28, ^{113}Cd, pH 8.0. Acquisition conditions were as in Figure 4. The protein concentration was 3 mM.

around the binuclear metal cluster by the heteronuclear NMR techniques allows a more restrained cluster structure to be entered in the data set used to calculate the 3D structure of GAL4(62*). For the cluster structure pictured in Figure 10, the Cd_2 cluster was entered in the XPLOR program as two fused tetrahedral Cd–S_4 complexes with the appropriate bridging ligands. The bond lengths were restrained at ±0.05 Å, while the bond angles were allowed to deviate by as much as 15° during the energy minimization of the surrounding polypeptide fold. The resulting cluster assumes a reasonable geometry with relatively small deviations from model Cd–S complexes. The sulfur atoms of C11 and C28 and the two Cd ions define a square with bond angles of ~90°. The Cd–S bond lengths range from 2.45 to 2.55 Å, and the Cd–Cd distance is 3.6 Å. Outside the bridging "square", there is moderate deviation from tetrahedral geometry with bond angles from 90 to 120°.

Both $Zn(II)_2$ and $Cd(II)_2$ derivatives of GAL4(62*) are accommodated in this structure. The loop arrangement with C11 and C28 as bridging ligands leaves the site with primary –S^- ligands from C11, -14, -21 somewhat more exposed to solvent. On the basis of the HMQC, the ^{113}Cd resonance for this site occurs at 669 ppm (Figure 3). The greater exposure of this site to solvent appears to explain why the ^{113}Cd resonance from this site undergoes some exchange modulation which can be detected at 44 MHz and is more readily exchanged for Zn(II) (Pan & Coleman, 1990a). This solvent exposure is also compatible with the observation that when a Zn–^{113}Cd hybrid is formed from the "native" GAL4(62*), the Zn(II) appears to be most stably bound to the C28, -31, and -38 site (707 ppm), while ^{113}Cd most readily exchanges out the Zn(II) bound to the C11, -14, and -21 site (669 ppm) (Pan et al., 1990b). That there are differences in conformation between the Zn(II) and Cd(II) clusters is best documented by the fact that the adjustment to the larger Cd(II) ion is accompanied by significant change in the torsional angles of the polypeptide chain around the cluster (residues 10–40) (Figure 9). The magnitudes of the changes in $^3J_{HN\alpha}$, -2 to -4 Hz, suggest that the changes in ϕ may be 20°–30° on the basis

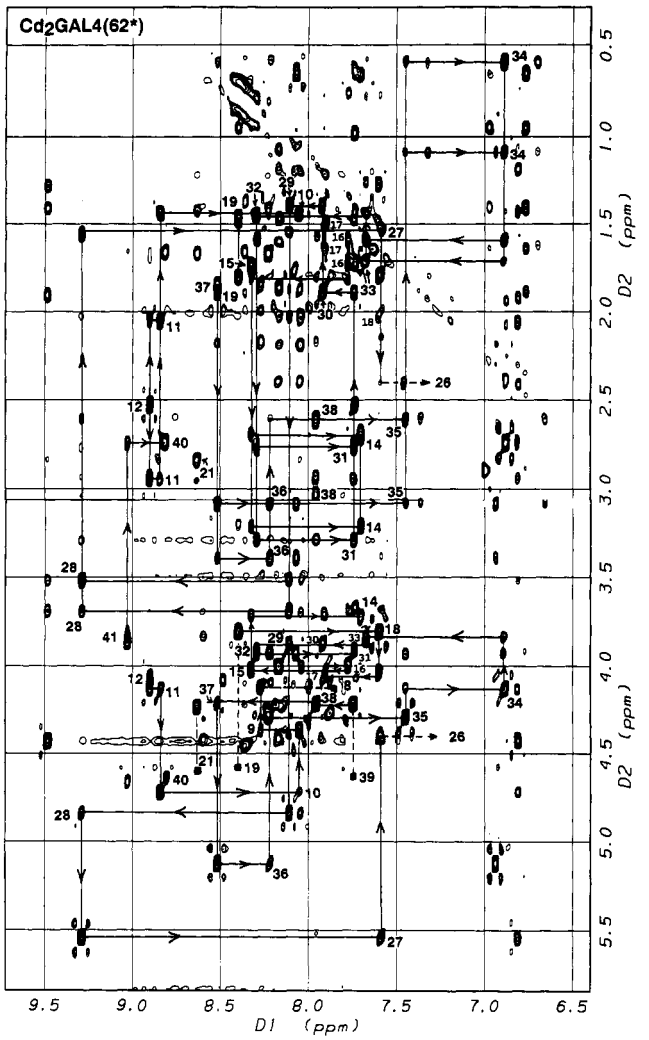

FIGURE 6: NOESY spectrum of the αNH and βNH region of $^{113}Cd_2$GAL4(62*). Assignment of the sequential αN(*i*,*i*+1) and βN(*i*,*i*+1) NOE contacts between residues within the binuclear cluster Glu8–Ser41 are shown by the lines. For clarity the (*i*,*i*) NOESY peaks are indicated by numbers only. The amino acid sequence is (E8)-QA(C11)DI(C14)RLKKLK(C21)SKEKPK(C28)AK(C31)LKNNWE(C38)RY(S41). The protein concentration was 15 mM, pH 6.0, at 35 °C.

of correlations of $^3J_{HN\alpha}$ with ϕ values taken from crystal structures (Wüthrich, 1986).

We have presented the heteronuclear coupling patterns and resonance positions of the Cys residues of GAL4(62*) both at pH 8 and at pH 6 for the ^{113}Cd derivatives in order to make the point that there appears to be very little change in the cluster arrangement or the conformation of Cd_2GAL4(62*) when shifting from neutral pH to pH values between 5 and 6; the latter necessary to slow NH proton exchange. In the case of metalloproteins, however, there is concern that increased proton–metal ion competition for the ligand donors may destabilize the protein at even moderately low pH values. Such destabilization does become a problem in managing the equilibrium between Zn_2GAL4(62*) and Zn_1GAL4(62*). It is apparent, however, that at the low pH values the presence of the metal ions is necessary to maintain the native structure since the chemical shift dispersion of the "fingerprint" region of the COSY spectrum of GAL4(62*) collapses when zinc is removed at pH 5.5 (data not shown).

The rapid simultaneous T_1 relaxation of both ^{113}Cd nuclei in $^{113}Cd_2$GAL4(62*) may reflect the cluster structure. CSA is likely to be a contributing relaxation mechanism for such short T_1's at 110 MHz, and it is true that the ^{113}Cd line width

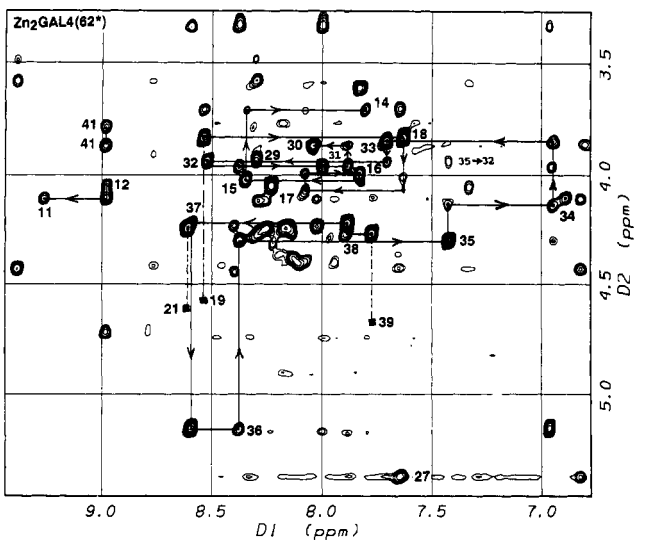

FIGURE 7: NOESY spectrum of the αNH region of Zn_2GAL4(62*). The αNH(*i*,*i*+1) connectivities are made for residues 11–12, 14–19, 26–27, and 30–39. One (*i*,*i*+3) αNH NOE is present between residues 32 and 35. The sample was 4 mM in protein, pH 5.4, 35 °C.

in GAL4(62*) is approximately the same, 110 Hz, as that observed for ^{113}Cd–gene 32 protein, a protein 3.7 times the molecular weight, where dipolar relaxation is a major contributor to T_1 (Giedroc et al., 1989). Whatever CSA is present, however, must have an equal effect on both ^{113}Cd nuclei in GAL4(62*). In contrast to the ^{113}Cd ions in GAL4, the T_1's of the two ^{113}Cd ions in the $^{113}Cd_2$ derivative of the glucocorticoid receptor have 10-fold different T_1's, 0.2–0.4 s for one and 2–3 s for the other (Pan et al., 1990a). The structure of the DNA-binding domain of this receptor shows the two metal complexes to occupy separate subdomains ~13 Å apart (Härd et al., 1990).

The coordination chemistry of GAL4 has proved to be more complex than we initially recognized. The highly cooperative binding of two ^{113}Cd(II) ions giving rise to distinct ^{113}Cd resonances established the ability of the DNA-binding domain of GAL4 to form a binuclear cluster (Pan & Coleman, 1989, 1990). While the native metal ion, Zn(II), can also form the binuclear cluster, one of these Zn(II) ions can easily be lost by dialysis against metal-free buffer, especially as low pH values. As argued above, this is most likely the ion coordinated to C14 and C21 as the terminal $-S^-$ ligands. The relative lability of the second Zn(II) ion requires considerable care in preparing Zn_2 derivatives at pH 6 or below. Dialysis at low pH always produces the Zn_1 derivative and even addition of extra Zn(II) to the protein at pH 5.5 does not always restore the second zinc. It is best to form the Zn_2 protein at pH 8 and then reduce the pH by dialysis against buffers contains at least 100 μM Zn(II).

The structures of both the Zn_2- and Cd_2GAL4(62*) protein are related, as can be deduced by the patterns and relative magnitudes of the NOE's (NN, αN, and βH) (Figures 6–8). While both bimetallo derivatives have short stretches in the N-terminal and C-terminal regions of the cluster where there are reasonably strong NN NOE's, the relatively large magnitudes of the αN NOE's in the same regions and the size of the αN–NH coupling constants suggest these peptide loops are distorted from an α-helical conformation in these two regions (Figure 9). On the other hand, the stable Zn_1GAL4(62*) not only shows substantial changes in proton chemical shifts, especially the NH protons, but its NN NOEs from residues 12–19 and 30–36 are all relatively strong and the αN NOE's for the same residues are weaker than in the

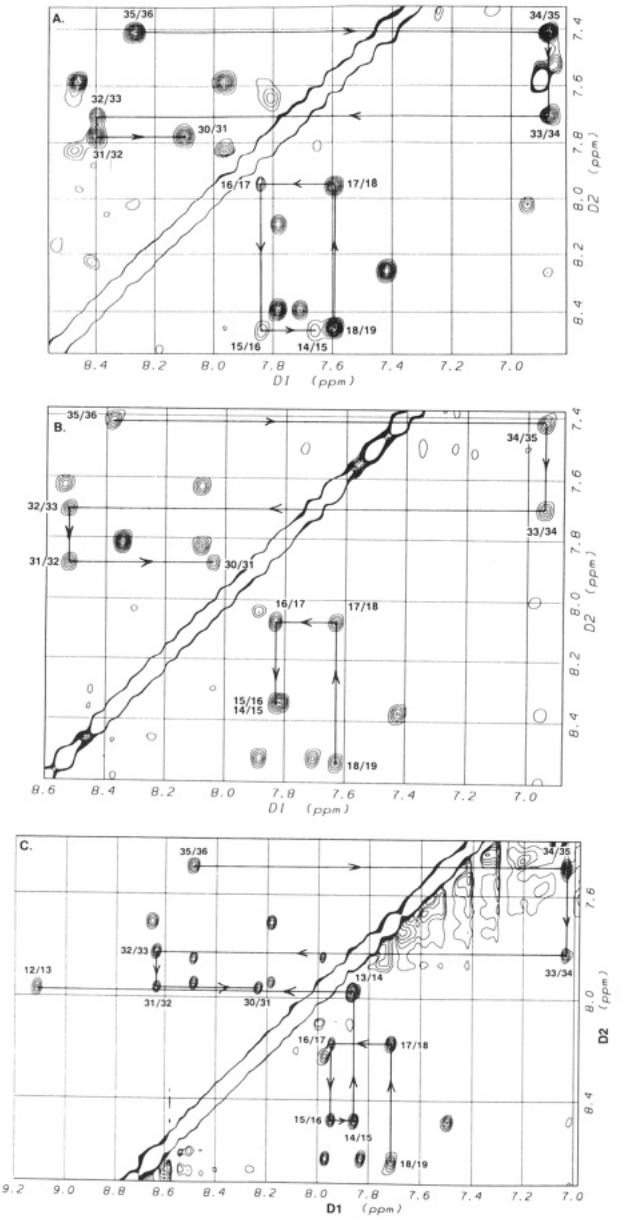

FIGURE 8: NOESY spectra for the NH–NH region of $^{113}Cd_2$GAL4(62*) (A), Zn_2GAL4(62*) (B), and Zn_1GAL4(62*) (C). Sample conditions were 15 mM $^{113}Cd_2$GAL4(62*), pH 6.0, 10 °C; 4 mM Zn_2GAL4(62*), pH 5.4, 35 °C; Zn_1GAL4(62*), pH 5.5, 25 °C. Note: NOESY spectra were taken at 10, 25, and 35 °C, and no substantial differences in the magnitudes of the NOE's or the NOESY connectivities were observed.

Zn_2 derivative (data not shown).

A recent report of a relayed HMQC spectrum on the ^{113}Cd derivative of a subdomain (residues 7–49) of GAL4 [GAL4-(43)] shows C11 and -28 to be the bridging ligands in the case of the smaller fragment as well (Gadhavi et al., 1991). While details of the ^{113}Cd cluster appear to be similar, the NH and αCH chemical shifts of the Zn(II) derivative of this same 43-residue subdomain reported earlier by the same investigators (Gadhavi et al., 1990) are significantly different from those we find for the same residues in Zn_2GAL4(62*) (Pan & Coleman, 1991). In fact, the pattern of NN NOE's and NH chemical shifts reported for ZnGAL4(43) by Gadhavi et al. (1991) fit very closely the NN NOE pattern we find for Zn_1GAL4(62*) (Figure 8C). Gadhavi et al. (1990) suggest that the regions of the polypeptides from residues 12–19 and 30–36 may be α-helical. Our data on the Zn_1Gal4(62*) suggest that these regions are likely to be α-helical as well in

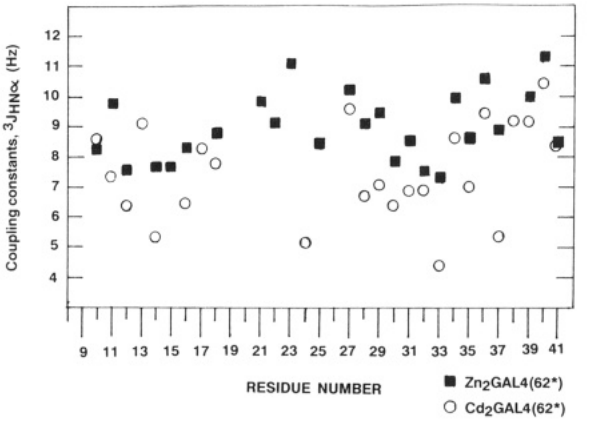

FIGURE 9: Plots of the coupling constants, $^3J_{HN\alpha}$, for Zn_2- (■) and Cd_2GAL4(62*)(○) in the region of residues 9–41. The coupling constants were measured from two-dimensional cross sections of NH–αCH cross peaks in the DFQ ^1H COSY of the Zn and Cd proteins at pH 5.4 and 6.0, respectively.

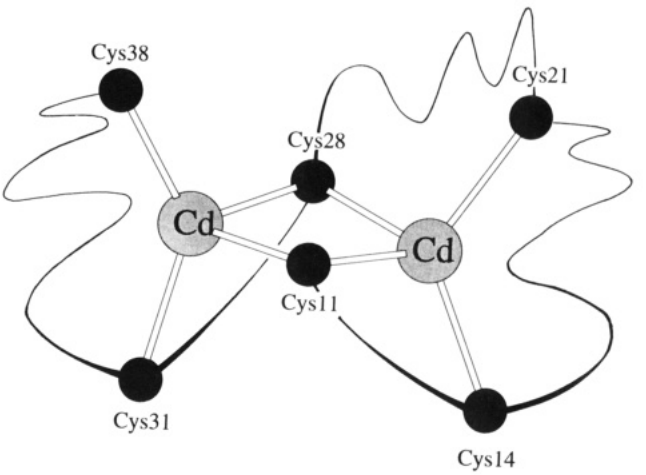

FIGURE 10: Configuration of the ^{113}Cd binuclear cluster of $^{113}Cd_2$GAL4(62*) taken from an energy-minimized structure of the protein refined from 2D NOESY data as described in the text. The wavy lines represent the three six-residue connecting loops, while the single curved lines represent the two-residue connecting loops between the Cys residues.

this form of the protein, although we have not determined a complete 3D structure as yet.

The DNA-binding domain of GAL4 clearly forms a binuclear Cd_2 cluster with Cys residues 11 and 28 as bridging ligands. This cluster in the case of Cd(II) can be said to be necessary for recognition and tight binding to the specific regulatory DNA sequence, UAS_G. The binding of two Cd(II) ions is so cooperative, in fact, that it appears that the Cd_2 protein is the only metalated species present at equilibrium, i.e., a 1:1 mixture of Cd(II)/protein is ~50% Cd_2 protein and ~50% apoprotein. Cadmium, however, is not the native metal ion, and cooperative formation of a binuclear Zn(II) cluster may not be so energetically favorable as in the case of Cd(II). A Zn_2GAL4(62*) species can be prepared which appears to have a structure similar to that of the corresponding Cd_2GAL4(62*) as judged by both 1D and 2D NMR criteria (Figures 6 and 7; Pan & Coleman, 1990a,b). However, GAL4(62*), GAL4(63), and GAL4(149*) derivatives containing between 1 and 1.4 zinc ions can be prepared rather easily by dialysis against metal free buffer (Pan & Coleman, 1989, 1990a,b). The absence of the characteristic apoprotein resonances in the 1D ^1H spectra of these samples strongly suggests that the majority of these species contain approximately one Zn(II). We are attempting to refine the 3D

Table I: Chemical Shifts and ^1H–^1H and ^1H–^{113}Cd Coupling Constants for Six Cysteines of GAL4(62*)

	chemical shift[a]			^1H–^1H coupling constants (Hz)[a]			^1H–^{113}Cd coupling constants (Hz)			
Cys	H_α	$H_\beta a$	$H_\beta b$	$J_{\alpha\beta}a$	$J_{\alpha\beta}b$	$J_{\beta a\beta b}$	$J_{\beta a Cd}669$	$J_{\beta b Cd}669$	$J_{\beta a Cd}707$	$J_{\beta b Cd}707$
				(A) $^{113}Cd_2$GAL4(62*) at 35 °C, pH 8.0						
C11	4.22	2.99	2.12	7	<2	14	20	11	nd	nd
C14	3.75	2.77	3.26	10	<2	14	31	16		
C21	4.64	2.95	2.95	–[b]	–[b]	–[b]	55	–[b]		
C28	4.94	3.73	3.60	11	10	15	nd	nd	25	10
C31	3.98	2.82	3.35	10	<2	14			31	16
C38	4.33[c]	3.04	2.67	11	<2	22			55	26
				(B) $^{113}Cd_2$GAL4(62*) at 35 °C, pH 6.0						
C11	4.15	2.96	2.08	7	<2	14	20	22	≈5[d]	≈5[d]
C14	3.75	2.72	3.23	10	<2	14	31	15		
C21	4.62	2.84	2.84	–[b]	–[b]	–[b]	55	–[b]		
C28	4.86	3.70	3.54	11	10	15	>5[d]	<5[d]	30	10
C31	3.94	2.77	3.31	10	<2	14			31	16
C38	4.23	3.02	2.63	11	<2	22			55	26
				(C) Zn_2GAL4(62*) at 35 °C, pH 5.4						
C11	4.12	2.88	2.15							
C14	3.73	2.73	3.17							
C21	4.65	2.84	2.84							
C28	4.67	3.60	3.50							
C31	3.98	2.75	3.25							
C38	4.29	3.04	2.55							

[a] Note that by definition β^a is the proton with the larger homonuclear spin–spin coupling to αH ($^3J_{\alpha\beta}a$) (Neuhaus et al., 1984). [b] Not obtainable due to lack of resonances or degeneracy of the chemical shifts [c] Chemical shift differs from that of $^{12}Cd_2$GAL4(62*) (H_α: 4.29). The reasons for such differences are not clear. [d] These values are estimated from the double-quantum ^1H–^{113}Cd correlation spectra.

structures of the Cd_2, Zn_2, and Zn_1 derivatives of GAL4(62*) to a small enough RMS deviation so that we can characterize the nature of the conformational difference between the three derivatives.

The observation of an equilibrium between a Zn_1 and Zn_2 species raises the question of whether at physiological levels of zinc such a zinc-induced conformational switch could have a significant effect on transcriptional activation. Both species bind to the UAS_G sequence and preliminary titrations by gel retardation assays suggest that the Zn_1GAL4(149*) binds to a single copy of the UAS_G sequence with higher affinity than the Zn_2 derivative (Basile and Coleman, unpublished data). As discussed above, metal ion exchange data suggest the single zinc is probably still coordinated to C28, -31, and -38. It is likely that the one zinc protein completes a tetrahedral sulfur coordination by utilizing one of the remaining three Cys as a ligand. Unfortunately Zn(II) is spectroscopically silent, and the structural data do not as yet suggest a likely choice for the fourth ligand. Coordination of a single Zn(II) ion does appear to allow a more helical conformation to be assumed by parts of the polypeptide backbone within the cluster of six cysteines of GAL4(62*). Binding of the second metal ion and formation of the binuclear cluster appears to lead to structural adjustments in the backbone which do not accommodate a α-helical conformation but give rise to a somewhat irregular structure with larger ϕ torsional angles (Figure 10).

Regulation of the transcription of genes for metal-containing proteins via the formation of a metal cluster in a regulatory protein has been well established in the case of the yeast metallothionein gene. The N-terminal DNA-binding domain of the transcription factor for this gene forms a copper cluster similar but not identical to that of yeast metallothionein itself (Furst et al., 1988). Thus the principle of a metal-dependent switch operating for the control of gene expression is well established. Extrapolation of this principle to a nonmetalloprotein for which the transcription of its gene is regulated by a Zn-containing transcription factor, thus making the metal ion concentration an additional factor in the control of gene expression, requires more physiological information than is presently available. The physiological significance of an equilibrium between a Zn_1 and a Zn_2 form of a Zn protein domain required for specific DNA binding of a transcription factor also requires further investigation of the binding of these two forms of the protein to DNA sequences containing 1, 2, or 4 copies of the UAS_G sequence as found in the upstream regions of genes responding to GAL4.

Registry No. Cys, 52-90-4; Zn, 7440-66-6; Cd, 7440-43-9.

References

Brunger, A. (1990) XPLOR *Manual*, Yale University, New Haven, CT.

Frey, M. H., Wagner, G., Vasak, M., Sorensen, O. W., Neuhaus, D., Wörgötter, E., Kägi, J. H. R., Ernst, R. R., & Wüthrich, K. (1985) *J. Am. Chem. Soc. 107*, 6847.

Furst, P., Hu, S., Hackett, R., & Hamer, D. (1988) *Cell 55*, 705.

Gadhavi, P. L., Raine, A. R. C., Alefounder, P. R., & Laue, E. D. (1990) *FEBS Lett. 276*, 49.

Gadhavi, P. L., Davis, A. L., Povey, J. F., Keeler, J., & Laue, E. D. (1991) *FEBS Lett. 281*, 223.

Giedroc, D. P., Johnson, B. A., Armitage, I. M., & Coleman, J. E. (1989) *Biochemistry 28*, 2410.

Giniger, E., Varnum, S. M., & Ptashne, M. (1985) *Cell 40*, 767.

Härd, T., Kellenbach, E., Boelens, R., Maler, B. A., Dahlman, K., Freedman, L. P., Carlstedt-Duke, J., Yamamoto, K., Gustafsson, J.-A., & Kaptein, R. (1990) *Science 249*, 157.

Johnston, M. (1987a) *Microbiol. Rev. 51*, 458.

Johnston, M. (1987b) *Nature (London) 328*, 353.

Johnston, S. A., Salmeron, J. M., & Dincher, S. S. (1987) *Cell 50*, 143.

Keegan, L., Gill, G., & Ptashne, M. (1986) *Science 231*, 699.

Ma, J., & Ptashne, M. (1987) *Cell 48*, 847.

Marczak, J. E., & Brandriss, M. C. (1990) *J. Mol. Cell. Biol. 11*, 2609.

Neuhaus, D. G., Wagner, G., Vasak, M., Kägi, J. H. R., & Wüthrich, K. (1984) *Eur. J. Biochem. 143*, 659.

Neuhaus, D. G., Wagner, G., Vasak, M., Kägi, J. H. R., & Wüthrich, K. (1985) *Eur. J. Biochem. 151*, 257.

Norwood, T. J., Boyd, J., Heritage, J. E., Soffe, N., &

Campbell, I. (1990) *J. Magn. Reson. 87*, 488.
Otting, G., & Wüthrich, K. (1990) *Q. Rev. Biophysics 23*, 39.
Pan, T., & Coleman, J. E. (1989) *Proc. Natl. Acad. Sci. U.S.A. 86*, 3145.
Pan, T., & Coleman, J. E. (1990a) *Biochemistry 29*, 3023.
Pan, T., & Coleman, J. E. (1990b) *Proc. Natl. Acad. Sci. U.S.A. 87*, 2077.
Pan, T., & Coleman, J. E. (1991) *Biochemistry 30*, 4212.
Pan, T., Freedman, L. P., & Coleman, J. E. (1990a) *Biochemistry 29*, 9218.
Pan, T., Halvorsen, Y.-D., Dickson, R. C., & Coleman, J. E. (1990b) *J. Biol. Chem. 265*, 21427.
Robbins, A. H., McRee, D. E., Williamson, M., Collett, S. A., Xuong, N. H., Furey, W. F., Wang, B. C., & Stout, C. D. (1991) *J. Mol. Biol.* (in press).
Wüthrich, K. (1986) *NMR of Proteins and Nucleic Acids*, John Wiley & Sons, New York.
Wörgötter, E., Wagner, G., & Wüthrich, K. (1986) *J. Am. Chem. Soc. 108*, 6162.

Activation of Bovine Rod Outer Segment Phosphatidylinositol-4,5-bisphosphate Phospholipase C by Calmodulin Antagonists Does Not Depend on Calmodulin†

Barry D. Gehm,‡,§ Richard M. Pinke,‡ Sylvie Laquerre,‖ James G. Chafouleas,‖ Donna A. Schultz,‡ David J. Pepperl,‡ and David G. McConnell*,‡

Department of Biochemistry, Michigan State University, East Lansing, Michigan 48824, and Department of Biochemistry, Bio-Mega, Incorporated, 2100 rue Cunard, Laval, Quebec, Canada H7S 2G5

Received August 6, 1991

ABSTRACT: Calmodulin antagonists stimulated phosphatidylinositol-4,5-bisphosphate phospholipase C in soluble and particulate fractions of bovine rod outer segments. Antagonists tested include trifluoperazine, melittin, calmidazolium, compound 48/80, W-13 [*N*-(4-aminobutyl)-5-chloro-1-naphthalenesulfonamide], and W-7 [*N*-(6-aminohexyl)-5-chloro-1-naphthalenesulfonamide]. All were effective, but W-7 was chosen for further characterization of the effect, which was most pronounced in the soluble fraction. Phospholipase C activity in the soluble fraction did not increase linearly with the quality of enzyme assayed, suggesting the presence of an endogenous inhibitor or an inhibitory self-association of the enzyme. W-7 appeared to counteract this inhibition, resulting in a linear activity–quantity relationship. Stimulation by W-7 was therefore largest when large amounts of crude enzyme were assayed and small or nil when small amounts were assayed. The effect of W-7 was also dependent on [Ca^{2+}], with half-maximal stimulation occurring between 0.1 and 1 μM. W-7 and W-13 were much more effective than their nonchlorinated analogues W-5 and W-12 at increasing phospholipase C activity. While this pattern of effectiveness is typical of calmodulin-mediated processes, the absence of any effect by added calmodulin and the retention of W-7 sensitivity by purified CaM-free enzyme argue against regulation by CaM. Octyl glucoside, a nonionic detergent, mimicked some of the effects of CaM antagonists, suggesting that the antagonists act by interfering with protein–protein interactions. It appears likely that CaM antagonists prevent an inhibitory multimerization or aggregation of at least one form of ROS phospholipase C.

We have previously reported (Gehm & McConnell, 1990) that bovine retinal rod outer segments (ROS)[1] contain both soluble and particulate PIP_2 phospholipase C activities which are strongly affected by Ca^{2+} concentration. Ca^{2+} is absolutely required, and half-maximal activity is obtained at concentrations of ~0.1 μM for the soluble fraction and ~3 μM for the particulate. These results prompted us to examine the possibility that phospholipase C activity in ROS is regulated by calmodulin (CaM), a widely occurring Ca^{2+}-dependent regulatory protein (Means & Dedman, 1980).

CaM is present in ROS in both soluble and membrane-bound forms (Kohnken et al., 1981), but its function in ROS is unknown. Since ROS contain endogenous CaM, our initial experiments employed CaM antagonists to evaluate a potential role for CaM in phospholipase C regulation. Unexpectedly, we found that CaM antagonists stimulate PIP_2 phospholipase C in both soluble and particulate ROS fractions, raising the possibility that ROS phospholipase C is inhibited by CaM. Such inhibition would be extremely significant, as phospho-

† This work was supported by National Science Foundation Grant BNS 84-17256 and National Institutes of Health Grant EY06065, by NIH Biological Research Support Grants from MSU's College of Osteopathic Medicine and an All-University Research Initiation Grant from MSU, and by a Group Grant in Molecular Endocrinology from the Medical Research Council of Canada (MRC).

* To whom correspondence should be addressed.
‡ Dept. of Biochemistry, MSU.
§ Completed this work in partial fulfillment of the requirements for a Ph.D. degree from MSU. Present address: Ben May Institute, University of Chicago, 5841 S. Maryland, Box 424, Chicago, IL 60637.
‖ Department of Biochemistry, Bio-Mega, Inc.

[1] Abbreviations: BAPTA, 1,2-bis(*o*-aminophenoxy)ethane-*N*,*N*,*N*′,*N*′-tetraacetic acid; BSA, bovine serum albumin; EC_{50}, 50% effective concentration; EGTA, [ethylenebis(oxyethylenenitrilo)]tetraacetic acid; calmidazolium, 1-[bis(4-chlorophenyl)methyl]-3-[2-(2,4-dichlorophenyl)-2-[(2,4-dichlorophenyl)methoxy]ethyl]-1H-imidazolium chloride; CaM, calmodulin; Hepes, *N*-(2-hydroxyethyl)piperazine-*N*′-2-ethanesulfonic acid; IC_{50}, 50% inhibitory concentration; PI, phosphatidylinositol; PIP, phosphatidylinositol 4-phosphate; PIP_2, phosphatidylinositol 4,5-bisphosphate; ROS, retinal rod outer segments; W-5, *N*-(6-aminohexyl)-1-naphthalenesulfonamide; W-7, *N*-(6-(aminohexyl)-5-chloro-1-naphthalenesulfonamide; W-12, *N*-(4-aminobutyl)-1-naphthalenesulfonamide; W-13, *N*-(4-aminobutyl)-5-chloro-1-naphthalenesulfonamide.

0006-2960/91/0430-11302$02.50/0